# Understanding Gibbsite Particles Interactions and Agglomeration Behaviour for Improved Bayer Process Crystallization

**Addai-Mensah, J.**
Ian Wark Research Institute, ARC Special Research Centre
University of South Australia, Mawson Lakes, Adelaide. SA 5095, Australia.

## Abstract

Aluminium trihydroxide (□-$AlOH)_3$) or gibbsite crystallization in alumina ($Al_2O_3$) refineries is a pivotal step in the Bayer process for commercial production of alumina and aluminium metal from bauxite ores. Since the crystal growth kinetics in supersaturated Bayer liquors at elevated temperatures (60-90 $^oC$) are notoriously slow, conditions conducive to rapid agglomeration of fine gibbsite crystals are sought for the production of coarse particles of commercial interest. This work focuses on studies performed to elucidate the reluctance of colloidal size gibbsite crystals to undergo rapid aggregation and agglomeration during crystallization. Seeded, isothermal batch crystallization of gibbsite from synthetic liquors were carried out in which the role of alkali metal ion ($Na^+$ versus $K^+$) and the incidental particle interactions were probed at 65 $^oC$. Interactions between gibbsite particles dispersed in supersaturated sodium and potassium aluminate liquors were quantified in terms of temporal interparticle forces (by Colloid probe AFM) and dispersion rheology. The results show that both particle aggregation and agglomeration processes were faster in sodium than potassium aluminate liquors. Furthermore, strong repulsive forces which are not due to electrical double layer but structural or electro-steric interactions, initially exist between gibbsite surfaces, delaying the on-set of aggregation and agglomeration. With time, the interparticle repulsion attenuated and completely disappeared, followed by development of adhesive particle interactions. The particle interaction forces and the rates of dispersion thixotropic structure, shear yield stress and visco-elastic moduli development were faster in sodium than in potassium liquors, consistent with the agglomeration rates. The findings underscore the important role the non- crystallizing alkali metal (($Na^+$ versus $K^+$) ion plays in the interfacial phenomena underpinning the Bayer process gibbsite agglomeration mechanism.

**Keywords:**
Gibbsite crystallization, agglomeration, aggregation, particle interactions, supersaturated caustic aluminate liquors

## Introduction

To date, most of the world's alumina ($Al_2O_3$) is commercially produced from bauxite ores via the Bayer process. An important step of the process involves the crystallization of gibbsite ($\alpha$-$Al(OH)_3$) from seeded, supersaturated caustic aluminate solutions at temperatures 60 - 90 $^oC$. Gibbsite crystal growth is inherently slow; hence rapid agglomeration is highly promoted for the production of coarse particles of commercial interest in the product's refining to alumina. Coarse gibbsite crystals produced under well defined alumina refinery crystallization conditions have been observed to be agglomerates comprising fine (e.g., < 20 $\mu$m), inter-grown crystals of pseudo-hexagonal tabular or prismatic morphology [1-4]. The agglomeration phenomenon involves an initial weak, secondary minimum aggregation step, followed by irreversible cementation [5-7]. Several studies focussing on the agglomeration mechanisms have been performed to unravel the effect of supersaturation, crystal growth rate, temperature and seed surface area [5-8]. Although significant advances have been made in the understanding and modelling of the overall agglomeration mechanism [5-8] to date, the aggregation process remains to be completely elucidated. In particular, the role played by alkali metal ions (e.g. $Na^+$ or $K^+$ ions originating from caustic soda used in bauxite ore digestion) in aggregate and agglomerate formation has not been fully probed. Recourse to the literature shows that alkali metal ion specific effect on gibbsite particle interaction forces in pregnant Bayer liquors exists [9-11]. Interfacial structure development, interparticle adhesion forces and network formation as revealed by colloid probe atomic force microscopy (AFM) and rheological studies, were observed to be greater in sodium than in potassium aluminate liquors [9-12]. Direct quantification of the influence of alkali metal ion and Al(III) relative supersaturation on gibbsite aggregation and agglomeration mechanisms is needed for complete understanding and characterization of gibbsite particle enlargement process.

The main aim of the present work was to investigate the specific influence of $Na^+$ and $K^+$ ions originating from caustic solution and Al(III) supersaturation on the aggregation of colloidal size gibbsite crystals in synthetic Bayer liquors at 30 $^oC$. This was achieved by probing the coagulation behaviour of colloidal size gibbsite particles dispersed in sodium and potassium aluminate solutions at different degrees of relative supersaturation by monitoring turbidity changes during isothermal batch crystallization.

## Models for particle aggregation

To quantify the aggregation behaviour, changes in an extensive property of the colloidal dispersion (e.g. turbidity) with time are commonly determined. The turbidity ($\tau$) of a colloid

can be conventionally defined in terms of the reduction in intensity (I) of a beam of light passing through an optical path length L of suspension of non-absorbing colloidal particles [13-16]:

$$\tau = -\frac{1}{L}\ln\left(\frac{I}{I_o}\right) \qquad \square\ \square\ \square$$

where $I_o$ is the incident light intensity and I is the transmitted light intensity. For a suspension of uniform particles, the turbidity may be defined simply as below [18]

$$\tau = N_T \pi a^2 Q_1 \qquad (2)$$

where $Q_1$ is a scattering coefficient, $N_T$ is total particle number per unit volume of suspension and a is the particle radius. The scattering coefficient depends greatly on the particle size, refractive index and the light wavelength (□ □ . When the particle size is greater than □ /10, $Q_1$ may be computed from Mie theory [16]. Anomalous diffraction approximation may also be used for $Q_1$ when the particle refractive index is not greatly different from that of the suspension medium for quite large particles [13-17]:

$$Q_1 = 2 - \frac{4}{\rho}\sin\rho + \frac{4}{\rho^2}(1 - \cos\rho) \qquad (3)$$

where □ = 2□ (m– 1) and □ = 2□ a /□ □ □ where □ is a dimensionless particle size, m is the relative refractive index which is the ratio of the refractive indices of the particle and suspension medium and □ is the irradiating light wavelength. For a suspension uniform spherical particles of radius a and solid volume fraction □ = 4□ Na$^3$/3, The specific turbidity □ /□ may be defined as:

$$\frac{\tau}{\phi} = \frac{3Q_1}{4a} \qquad (4)$$

Equation 1 indicates that for small particles, the turbidity will initially increase with increasing particle size upon aggregation, whilst Equation 4 shows the specific turbidity to vary inversely with particle size. Consequently, a positive change in turbidity as the particles start to aggregate, followed by a systematic decrease upon further aging where coarser particles are eventually formed and Q becomes substantially constant, are expected. For a fairly dilute dispersion with an initial primary particle concentration of $N_o$, where the particles may be considered to be "free" as opposed to "restricted" in space, the initial rate of decrease of the total particle concentration, $N_T$, due to aggregation can be calculated as:

$$\left(dN_T/dt\right)_{t\to 0} = -k_1 N_o^2 \qquad (5)$$

where $k_1$ is the initial aggregation rate constant.

Considering Equations 2 – 5, the initial rate of increase turbidity from an aggregating suspension due to doublets formation can be related to the initial particle number as [16-18]:

$$\left(d\tau/dt\right)_{t\to 0} = \left(C_{11}/2 - C_1\right)k_{11}N_o^2 \qquad (6)$$

where $C_1$ and $C_{11}$ are constants related to the scattering sections of the singlets and doublets, respectively, $k_{11}$ is the rate constant of doublets which is the rate constant for primary particle collisions and $(C_{11}-2C_1)\, k_{11} / 2 = k_1$

In the present work, the attenuation of visible radiation ( = 488 nm) is due to scattering and is referred to as absorbance (A), considered to be approximately equal to turbidity, [13, 18]. It is pertinent to note that the absorbance measurements reflect the attenuation of incident visible radiation by Mie scatterers rather than the absorption of radiation by particles. Furthermore, the primary gibbsite particles do not have spherical shape as assumed in the theoretical derivation of Equations 2 – 6. However, the meaningful results obtained from the turbidity (absorbance) data analysis and their high consistency or strong agreement with crystal number and size distribution data from parallel crystallization runs, suggest that the sphericity factor does not cause a significant problem.

**Experimental Methods**

Optically clear, synthetic, supersaturated sodium and potassium aluminate solutions which were twice filtered through 0.2 m membrane were used in this study. They were prepared from aluminium metal (99.99 % pure, 0.01 % Si, Merck, Australia); NaOH (99.0 % pure, 1.0% $Na_2CO_3$, Merck, Australia); KOH (85.0 % pure, 13.5 % $H_2O$, 1.0% $K_2CO_3$ and 0.5 % Na, Merck, Australia) and Milli-Q water (surface tension 72.8 mN $m^{-1}$ at 20 $^oC$, specific conductivity < 0.5 S $cm^{-1}$). NaOH is the alkali so far used by industry for bauxite digestion. Fresh solutions containing 4.0 M caustic [NaOH or KOH] and 2.48 - 3.23 M Al(III) with initial Al(III) relative supersaturations ( were 1.15, 1.30, 1.53 and 1.80 at temperatures 65 or 75 $^oC$ were prepared and used. Colloidal sized gibbsite particles (0.1 – 3 m) with BET surface area 6.8 $m^2\ g^{-1}$ and refractive index 1.58 were prepared by secondary nucleation using seeded, supersaturated sodium and potassium aluminate liquors. Seed loading of 0.25 g $dm^{-3}$ solution was used.

In the present aggregation studies, a baffled, well-sealed, 2.5 $dm^3$, 316 stainless steel vessel was used for isothermal batch crystallization. A central, 4-blade, 45 $^o$-pitch, 4.5 cm turbine impeller driven by a 70 W, motor provided a constant agitation speed in the crystallizer. A thermocouple sensor was fitted through the lid of the crystallizer which was submerged in a 15 $dm^3$, thermostatically-controlled oil bath, maintaining a constant temperature to within ± 0.05 $^o$C. The crystallizer suspension was initially homogenized at 700 rpm for 10 min to ensure a high degree of uniformity (confirmed by turbidity measurements) and thereafter maintained at agitation rate of 150 ± 2 rpm throughout the experiments lasting 6 h. Aliquots of the suspension were isokinetically removed at various time intervals with a prefabricated syringe and placed into a caustic-resistant plastic cuvette for absorbance (turbidity) measurements at 65 $^o$C and □ = 488 nm using a Carry 1E UV-Vis spectrophotometer. Colloid probe atomic force microscopy (AFM) Nanoscope III (Digital Instrument Santa Barbara, CA. USA) fitted with calibrated $SiN_4$ cantilever and a special glass fluid cell was used in measuring the interaction forces acting between gibbsite particles across synthetic Bayer liquors at 65 $^o$C.

Dissolved Al(III) and NaOH or KOH concentrations were determined by inductively coupled plasma atomic emission spectroscopy (ICP-AE, Spectro Analytical Instruments, SIM-SEQ) and electrodeless conductivity technique [19]. Scanning electron microscopy (SEM) and X-ray powder diffraction (XRD) analyses on the solid samples were performed using an SEM Camscan CS44 (Cambridge, UK) and XRD diffractometer (Philips PW1050 X-ray generator equipped with Sietronic data collection), respectively.

**Results And Discussions**

Typical orthokinetic aggregation behaviour of colloidal size gibbsite dispersed in sodium and potassium aluminate liquors is exemplified by the variation of turbidity (absorbance) with time in Figures 1-4. The data indicate the absence of an induction time and a marked increase in turbidity which reached a maximum with time, followed by a systematic attenuation upon further aging. The time required to reach maximum turbidity apparently decreased with increasing initial Al(III) relative supersaturation and was significantly less in $Na^+$ than in $K^+$ based suspensions. The absence of induction time for aggregation may be attributed to the high crystal-crystal contacts due to the high initial particle number density of $10^{15}$ number.$m^{-3}$ solution and micro-mixing provided at 150 rpm agitation rate. The aggregating rate of

crystals is noted to be faster in $Na^+$ based than $K^+$ based suspensions. The findings agree well with those obtained by colloid-probe AFM and rheological studies [9-12] which showed that the development and growth of adhesive interfacial layers or interparticle attractive forces were faster in $Na^+$ than in $K^+$ based liquors.

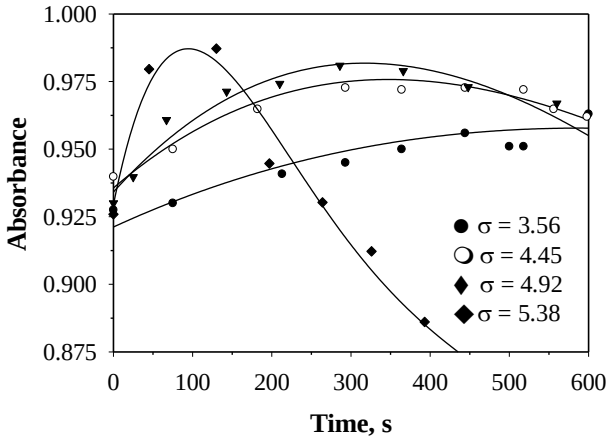


**Figure 1.** Turbidity of a gibbsite – sodium aluminate suspension as a function of time at different □ with seed charge = 0.25 g dm$^{-3}$ solution and at 65 $^{o}$C.

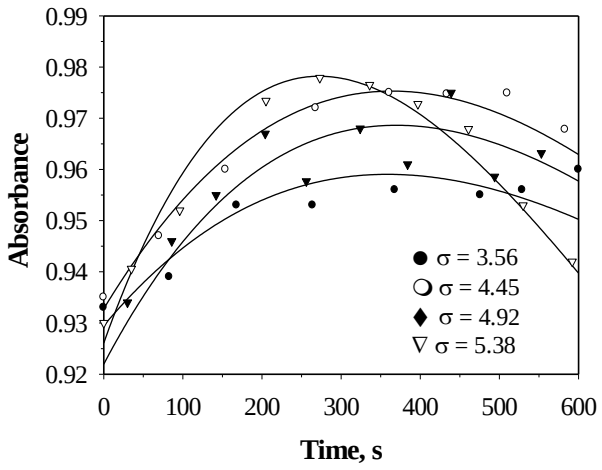


**Figure 2.** Turbidity of a gibbsite – potassium aluminate suspension as a function of time at different □ with seed charge = 0.25 g dm$^{-3}$ solution and at 65 $^{o}$C.

To quantify the aggregation kinetics and their dependence upon □ □ and□ alkali metal ion type, the slopes of the tangents to the initial absorbance versus time curve $(dA/dt)_o$ were first determined. The values obtained indicated that the initial rates of absorbance varied linearly with □ . For thesodium based suspension, when □ increased from 3.6 to 5.4, the initial rate of

change of absorbance increased by ~ 3 times but for the potassium based suspensions, the rate approximately doubled in the same □ □ range. In the □ □ range investigated, the $Na^+$ based suspension has an initial rate of absorbance 1.2 – 1.5 times larger than that of the $K^+$ based suspensions.

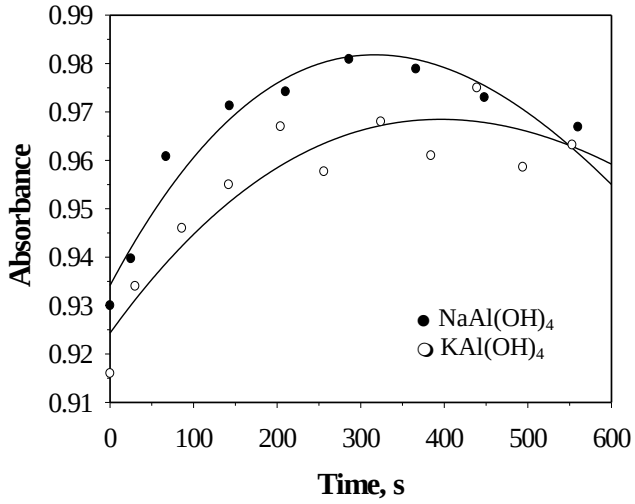


**Figure 3.** Turbidity of a gibbsite – caustic aluminate suspension as a function of time at □ □ □ = 4.9 seed charge = 0.25 g $dm^{-3}$ solution and at 65 $^oC$.

.

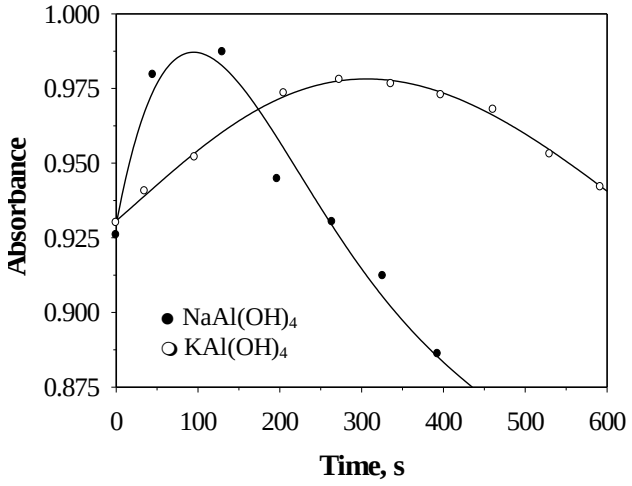


**Figure 4.** Turbidity of a gibbsite – caustic aluminate suspension as a function of time at □ □= 5.4 (B) and 65 $^oC$. Seed charge = 0.25 g $dm^{-3}$ solution.

The initial aggregation rate constant, $k_1$, was estimated on the basis of Equation 6 from the initial changes in absorbance measurements $(dA/dt)_o$. The $k_1$ values increased linearly with

increasing  and were greater in sodium than in potassium based suspensions as shown in Figure 5. This result is in agreement with reported gibbsite aggregation studies using rheological methods [12], where the aggregation rate was found to proportional to the relative supersaturation to a power of 1. The higher $k_1$ values obtained from sodium based suspensions suggest that the sticking probability of the particles is substantially greater in the presence of $Na^+$ ions, in comparison with $K^+$ ions, facilitating aggregation. These findings strongly concur with those of previous studies showing that gibbsite particle-solution interfacial structure development leading to attractive/adhesive forces is greater in $Na^+$ than in $K^+$ aluminate liquors [9-11].

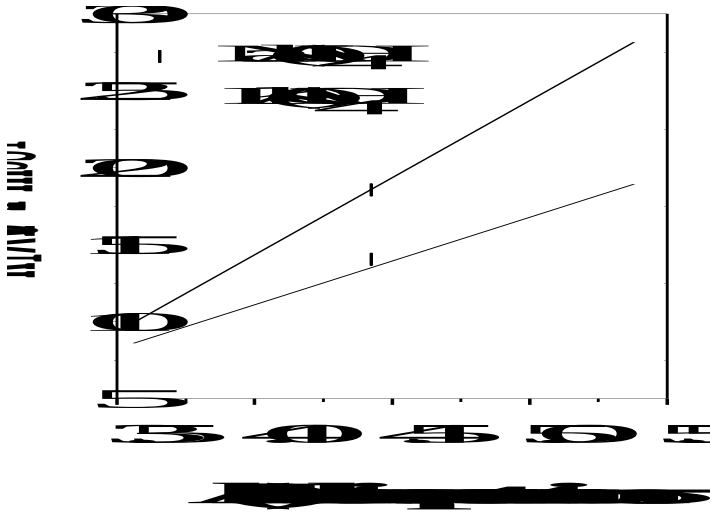

**Figure 5.** Initial aggregation rate constant $k_1$ as a function of Al(III) relative supersaturation  of caustic aluminate solution at 65 $^oC$ with initial particle number concentration of $10^{15}$ $No.m^{-3}$ solution**.**

The linear dependence of the initial aggregation rate constant on Al(III) relative supersaturation of both $Na^+$ and $K^+$ based suspensions is in contrast with a fourth order dependence gibbsite agglomeration kernel upon supersaturation previously reported [6,7]. The current observation indicates that aggregation process is substantially a physical interaction mechanism whereas agglomeration involving a cementation process is driven by a surface Al(III) polycondensation, chemical reaction whose rate is strongly dependent upon Al(III) supersaturation. Absolute viscosities of $Na^+$ based Bayer liquors are higher than that of $K^+$-based liquors [19]. It has been reported that high solution viscosity may lead to

hydrodynamic coupling or repulsion between colloidal gibbsite particles upon approach at high velocity [20]. On the hand, it is pertinent to note that upon glancing collision between two gibbsite crystals, a high solution viscosity will act to prolong the contact time, thereby facilitating attractive van der Waals attraction and cementation between particles. It appears that the prolonged interparticle contacts due to higher viscosity of $Na^+$ based liquors is more dominant than any hydrodynamic repulsion effect on the particle interactions.

**Interactions forces between Gibbsite crystals under Bayer conditions**

Typical size-normalised force (F/R) - separation data measured at a fresh gibbsite basal (001) face in fresh caustic aluminate solutions is shown in Figure 6. The results indicate the existence of strong inter-particle repulsion over a separation of 40 nm in Bayer liquors, initially. The observed repulsion is not of electrical double layer in origin as the Debye length in this system is < 0.1 nm due to the high ionic strength. Under similar solution conditions, structural or electro-steric repulsion develop initially, the magnitude of which was found to be 20% higher in $NaAl(OH)_4$ than $KAl(OH)_4$ solution. Similar trends with 30% lower, initial repulsion were observed at the non-(001) face. The results were satisfactorily reproducible for a fresh gibbsite - Bayer liquor system.

A.

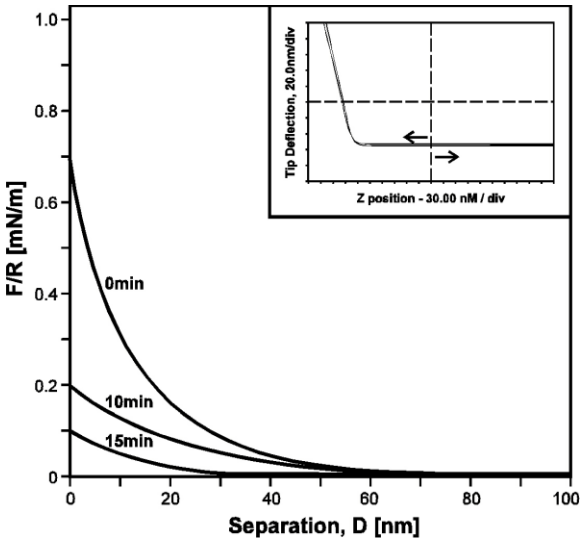


**Figure 6.** F/R as a function of separation measured at a fresh (001) gibbsite crystal face in fresh $NaAl(OH)_4$ solution ([Al] = 2.9 M, [NaOH] = 4.0 M) at 65 °C, t = 0 - 1 h and a scan rate of 0.59 □ m $s^{-1}$.

The existence of unusual, non-DLVO repulsive forces in colloidal dispersion of gibbsite – sodium aluminate solution at high ionic strength (~ 4.0 M) has been reported (Addai-Mensah et al., 1997). At high ionic strength and low particle approach velocity 0.59 □ m $s^{-1}$ used, the contributions of both electrostatic and hydrodynamic forces to repulsion may be completely discounted. The interparticle repulsion is consistent with the presence of a repulsive "electrosteric" or "structured" layer of 20 nm thickness at the gibbsite-solution interface. Furthermore, the sizes of the asperities on the surfaces of the gibbsite particles give rise to surface roughness which renders the detection of van der Waals forces unlikely. Electro-steric stabilization may result from the development of Al(III)-containing, polymeric layer around the crystals. Given the high supersaturation of the solutions, a reasonable tendency for surface adsorption of a multitude of $Al(OH)_4^-$ ions to occur and initiate interfacial structuring around individual particles prior to crystalline layer growth is expected, even at temperatures as low as 65 °C. The results show that, subsequent to the disappearance of steric repulsion, both the thickness of the adhesive interfacial layer, believed to be due to a more structured Al(III)-polymeric structure, and the extent adhesion increased systematically with time.

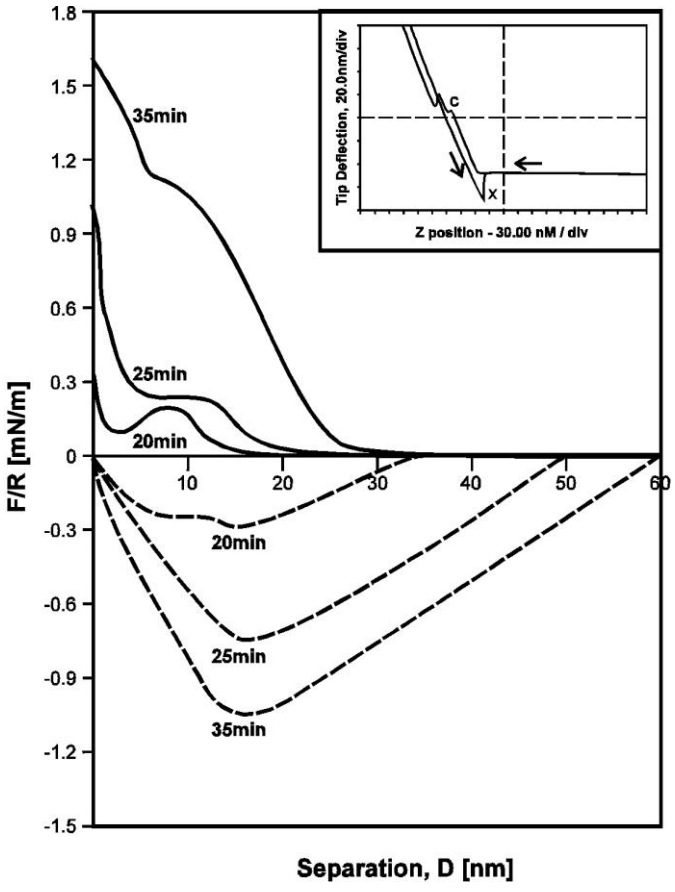


B.

**Figure 7:** F/R as a function of separation measured at aging, (001) gibbsite crystal face in $NaAl(OH)_4$ solution ([Al] = 2.9 M, [NaOH] = 4.0 M, A/C = 0.7, C = 212 g $dm^{-3}$ $Na_2CO_3$) at 30°C and a scan rate of 0.59 □ m $s^{1}$. Top curves = approach, and corresponding bottom curves = retreat of particles measured at the same times.

On further aging (>0.25 h), inter-particulate adhesion occurred with the emergence of an adhesive layer at the particle-solution interface (Figures 7, bottom curves). A significant hysteresis in the force-separation curves, indicative of inter-particle adhesion or attraction, was observed. The top and bottom curves of Figure 7 obtained at 35 min follow on from the last curve in Figure 6, recorded after 15 min at the (001) face. The top curves describe the forces observed on approach of particles whiles the bottom curves, bearing indicate the corresponding forces on withdrawal of the particles measured at the same time. The approach curves (top) indicate the appearance and systematic growth new barriers on approach of the crystals. The shape and size of the approach curve describe the loading forces needed to compress the interfacial layer and push the two particles further into hard contact. The separation range spanned by the (approach) force curve gives the thickness of the interfacial layer forming at the particle surface. The extent of adhesion is indicated by the depth of the adhesion well (bottom curves). These observations suggest increasing structuring and densification of the Al(III)-containing interfacial layer occur with aging. The development of the adhesive layer indicates that a systematic increase of interfacial layer structuring and with time as part of the seed crystal growth process and also precursor to agglomeration and granule growth. Higher crystal agglomeration rates may therefore be predicted for sodium based- rather than potassium based-liquors. The observed force-separation relationships are consistent with the previous gibbsite colloid stability data obtained from colloid probe AFM, rheological and coagulation (9-12, 20) studies.

SEM photomicrographs revealed that the colloidal size primary crystals precipitated from sodium aluminate liquors were pseudo-hexagonal tablets whilst those from potassium aluminate liquors were elongated hexagonal prisms (Figure 6 A and A'). Subsequent to their use as seeds, the particles underwent crystal growth and agglomeration (aggregation and cementation) over 6 h of crystallization. The agglomerates resulting from intergrowth of primary crystals in sodium aluminate liquors after 5 h were in 70 – 100 □ m size range (Figure 6 C) whilst those from potassium aluminate liquors were in 20-50 □ m size range (Figure 6 C'). These trends reflect alkali metal ion-specific, interfacial structure development

and particle interactions prior to cementation. Findings similar to the above have been observed in further work being carried out at the present at higher temperatures 65 and 75 $^{o}$C.

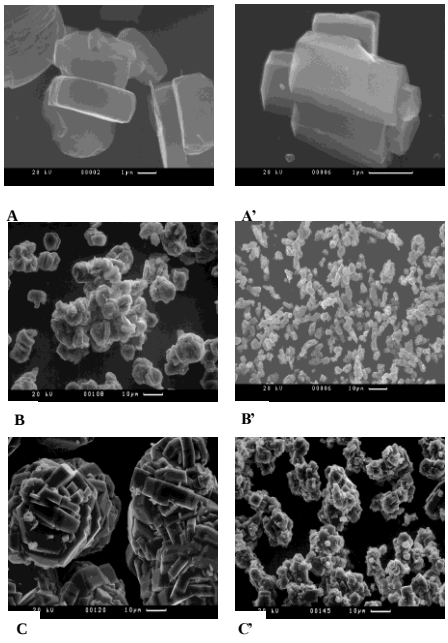


**Figure 8.** Scanning electron micrographs of crystals undergoing crystallization in sodium (A-C) and potassium (A'-C') aluminate solutions ([Caustic] = 4 M, □ = 1.53 and [Caustic]/[Al(III)] = 1.37) at 65 $^{o}$C and time t = 0 h (A and B), 4 h (A' and B') and 5 h (C and C'). Scale - A: 3 mm ⇔ 1 □ m; A': 7 mm ⇔ 1 □ m; B, B", C & C' 3 mm⇔ 10 □ m.

## Conclusions

Under orthokinetic conditions, the presence of $Na^{+}$, in contrast with $K^{+}$ ions, in synthetic, supersaturated caustic aluminate liquors significantly enhanced colloidal gibbsite particle size enlargement, albeit after an induction period, via aggregation, followed by cementation. The initial aggregation rate constant showed a linear dependence on Al(III) relative supersaturation and was higher for $Na^{+}$- than $K^{+}$-based liquors. These indicate the dominance of weak particle interactions, reflecting aggregation rather than agglomeration, between gibbsite crystals of colloidal dimensions. Furthermore, strong, supersaturation and alkali metal ion-mediated interfacial structuring is demonstrated to develop as part of gibbsite crystal growth process, impacting on the temporal inter-particle forces which emerged. The findings show that the initial orthokinetic aggregation and the subsequent cementation of gibbsite crystals, which underpin the agglomeration mechanism, are faster in sodium than in potassium aluminate liquors and greater at higher than lower Al(III) supersaturation. There is

therefore considerable merit for the alumina industry to use NaOH rather KOH to extract gibbsite from bauxite ores.

## REFERENCES

1. Misra, C., (1970). The Precipitation of Bayer Aluminium Trihydroxide, Ph.D. Dissertation, University of Queensland.
2. Wefers, K. and C. Misra, (1971) Oxides and Hydroxides of Aluminium, Alcoa USA,
3. Misra, C. and E. T. White, (1987). AIChE Symp. Series 438, **67(110)**, 53-65.
4. Addai-Mensah, J., (1997). Miner. Eng., **10(1)** 81.
5. Low, G. C., (1975). Agglomeration Effects in Aluminium Trihydroxide Precipitation, Ph.D. Dissertation, University of Queensland.
6. Halfon, A. and S. Kaliaguine, (1976). Canadian J. Chem. Eng., **54** 168.
7. Ilievski, D. and E. T. White, J. Chem. Eng. Sci., **49(19)** 3227 (1994).
8. Seyssiecq, I., S. Veesler, R. Boistelle and J. M. Lamerant, (1998). Chem. Eng. Sci. **53(12)** 2177
9. Addai-Mensah, J., C. A. Prestidge and J. Ralston, (1999). Miner. Eng., **12(6)** 655.
10. Addai-Mensah, J. and J. Ralston, (1999). J. Colloid Inter. Sci., **215** 124.
11. Prestidge, C. A., I. Ametov and J. Addai-Mensah, (1999). Colloids and Surfaces, **157** 137.
12. Prestidge, C. A. and I. Ametov, (2000). J. Crystal Growth, **209** 924.
13. Elimelech, M., J. Gregory, X. Jia and R. A. Villiams, (1995). Particle Deposition and Aggregation: Measurement, Modelling and Simulation. Butterworth-Heinemann Ltd., London.
14. Kerker, M., Chap. 9: The Scattering of Light and Other Electromagnetic Radiation. In Scattering by Liquids, E. M. Loebl (Ed.), Academic Press. New York**,** 487 (1969).
15. Sonntag, H. and K. Strenge, Coagulation Kinetics and Structure Formation, Plenum, NY., (1987).
16. Van de Hulst, H. C., Light Scattering By Small Particles, Dover Publications, Inc., NY (1957).
17. Maroto, J. A. and F. J. de las Nieves, (1997). Colloids Surf., **213**, 1148-1155.
18. Hiemenz, P. C. and R. Rajagopalan, (1986). Principles of Colloid and Surface Chemistry. Marcel Dekker, New York.
19. Li, J., J. Addai-Mensah, and C. A. Prestidge, (2000). J. Chem. Eng. Data, **45**(4) 665

20. Addai-Mensah, J., J. Dawe, R. Hayes, C. A. Prestidge, and J. Ralston, (1998). J. Colloid Inter. Sci., **203** 115.